

Optimizations, Stability and Physics Enhancements in the IMAS-compatible Multi-Mode Anomalous Transport Model

T. Rafiq, C. Wilson, J. Weiland, E. Schuster, A. Pankin

Lehigh University, Bethlehem, Pennsylvania, USA

Introduction

The Multi-Mode Module (MMM) is a physics-based model designed for multi-species, multi-fluid, and multi-mode anomalous transport calculations in tokamak discharges [1]. It is used in the integrated modeling code TRANSP for time-dependent simulations [2], computing profiles for anomalous electron and ion thermal transport, electron particle transport, impurity transport, and toroidal and poloidal momentum transport. These profiles predict electron and ion temperatures, electron density, and momentum rotation in tokamak plasmas. MMM incorporates various physical mechanisms to simulate complex plasma interactions and predict anomalous transport exceeding neoclassical theory predictions. It is noted for its comprehensive physics basis, computational efficiency, verification against gyrokinetic codes, validation across diverse experimental scenarios, and adaptability for both predictive simulations and control applications. MMM consistently matches gyrokinetic simulation results [3, 4], grounding its predictions in fundamental physics, and achieves these results using significantly less computational time. The model's flexible structure allows for the inclusion of new physics, making it adaptable to new findings and experimental data. MMM's well-defined interface facilitates porting to integrated modeling codes like TRANSP, ASTRA, and IMAS, enhancing data exchange and integration within the fusion research community. MMM's computational efficiency is crucial for real-time control applications, optimizing tokamak scenarios, and quantifying experimental data uncertainties.

Model Description

The model has been updated to version 9.1 (MMM 9.1), now integrated into the TRANSP code for predictive modeling and cross-verification with gyrokinetic codes and experimental data. Significant improvements in accuracy, stability, speed, and physics basis enhance its value for spherical and conventional tokamaks. The model includes: (i) A Weiland model for transport driven by ion temperature gradient, trapped electron, kinetic ballooning, peeling, and high mode number MHD modes [5]. (ii) A new electromagnetic electron temperature gradient mode (ETGM) model for electron thermal transport [6]. (iii) A microtearing mode (MTM) model for transport driven by electron temperature gradient in collisionless and collisionality regimes [7]. (iv) A drift resistive inertial ballooning mode (DRIBM) model for transport driven by gradients, electron inertial effects, and inductive effects [8]. MMM accounts for the stabilizing effects of $\mathbf{E} \times \mathbf{B}$ flow shear on plasma turbulence, crucial for accurately predicting fusion device performance.

The growth rate of all modes, except MTM, is reduced by subtracting the flow shear, as MTM is less influenced by it in gyrokinetic simulations. MMM 9.1 introduces updates to the Weiland model, including isotopic effects, a viscosity term, a new effective magnetic shear accounting for plasma shaping, and a uniform correlation length for both electron- and ion-scale modes. The Weiland component now runs over five times faster than the previous version. The older empirically based ETG model is replaced by the new ETGM model, incorporating geometry dependence, isotopic effects, impurity dilution effects, and $k_{\theta}\rho_s$ to find the most unstable mode at each magnetic flux surface. The upgraded MTM solver is significantly faster and now includes isotopic effects. The improved DRIBM component includes geometry dependence, $k_{\theta}\rho_s$ scan, and a new set of matrix equations. MMM 9.1 is more than ten times faster than its predecessor as a stand-alone program and successfully completes runs on machines where previous versions struggled within TRANSP. The MMM standalone module takes about 70 ms to calculate all electron and ion scale modes and their six diffusivities or transport fluxes for a single time slice, making it suitable for predicting profiles for advanced and long-pulse tokamaks, including EAST, KSTAR, ITER, and the Fusion Pilot Plant.

Optimizations and Stability

The MMM9.1 code optimizes the Weiland model to reduce the number of eigenvalue solver calls, thereby significantly decreasing runtime. The number of solver calls is reduced by 80% by focusing on the most unstable mode and eliminating less likely modes. The optimized profiles can be seen in Fig. 1. The input data comes from DIII-D discharge 118341, and the $E \times B$ flow shear effects were turned off. These optimizations maintained accuracy with negligible error and resulted in a more than two-fold increase in computational efficiency compared to MMM8.2.

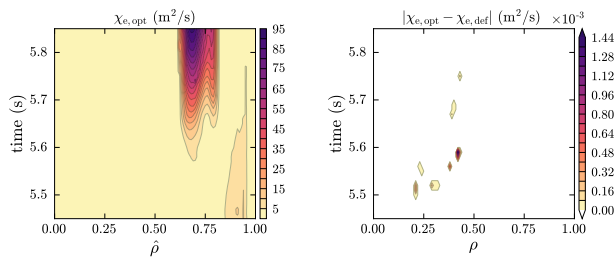


Figure 1: Optimized (opt) χ_e profile over time and position, and absolute differences between optimized (opt) and default (def) profiles. Optimized settings required only 44.2% as many eigenvalue solver calls as the default.

In the MTM case, a scan over $k_y\rho_s$ values is carried out to calculate diffusivity, with each scan requiring a call to the complex cubic solver, which dominates the runtime. To optimize MTM, minimize solver calls are aimed at obtaining precise results with fewer $k_y\rho_s$ scans. Since smaller $k_y\rho_s$ values significantly impact diffusivity calculations, precision is improved by refining these values instead of the entire range. This is achieved using an exponential function to space out $k_y\rho_s$ values, unlike the linear spacing in MMM v8.

Figure 2 shows that 100 exponentially spaced scans provide better diffusivity precision than

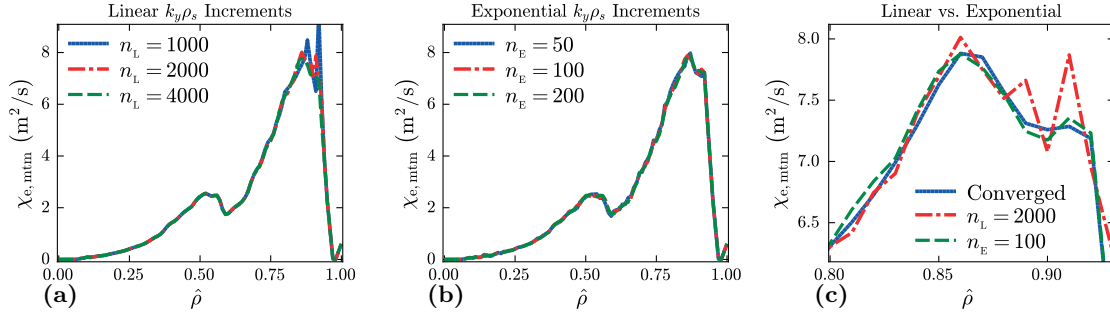


Figure 2: Convergence comparison of electron thermal diffusivity produced by the MTM model using (a) Linear $k_y \rho_s$ increments using n_L segments, (b) Exponential $k_y \rho_s$ increments using n_E segments, and (c) $n_L = 2000$ linear segments and $n_E = 100$ exponential segments against the converged result (10^6 linear segments). Data from NSTX-U discharge 121123 at $t = 11.8$ s.

2000 linearly spaced scans, significantly reducing run times. A limitation with the PT-Solver is encountered in the TRANSP code, which cannot handle negative diffusivities. Consequently, negative diffusivities are disabled in TRANSP-MMM predictive simulations, affecting the accurate prediction of experimental profiles in discharges with significant thermal and momentum pinches. Figure 3 displays MMM stand-alone predictions for electron particle transport using input from the NSTX 129016A04 TRANSP run. Disabling negative diffusivities affects predicted electron particle flux. While PT-Solver doesn't accept negative diffusivity, it allows both positive and negative convective velocities. Thus, negative diffusivity can be represented by converting them to convective velocities. Improving parameter ranges, adopting a uniform correlation length, and addressing negative diffusivities aim to enhance MMM's ability to capture plasma behavior while maintaining computational efficiency and stability.

Verification and Validation

Components of MMM, such as the ETGM [6] and MTM [7] models, are verified against gyrokinetic simulations. Good agreement is achieved between MTM-MMM and MTM-CGYRO results for both the real frequency and growth rate of the modes [3]. The ETG-MMM model accurately reproduces the real frequency of ETG-CGYRO modes, matching the magnitude of the most unstable mode in the $k_{\theta} \rho_s$ spectrum, though it stabilizes earlier [4]. This discrepancy is attributed to the inclusion of FLR effects in ETG-MMM. A large-scale validation exercise demonstrated MMM's ability to reproduce a wide range of conventional tokamak profiles from EAST, KSTAR, JET, and DIII-D, as well as low aspect ratio NSTX profiles [9, 4]. The validation data included scans over gyroradius and q_{95} values, and various plasma conditions such as ohmic, L-mode, and H-mode plasmas, with different density, collisionality, β_p , β_N , and ITB long-pulse scenarios. The study found an average RMS deviation of 9.3% for predicted electron temperature and 10.5% for ion temperature, within the experimental measurement error

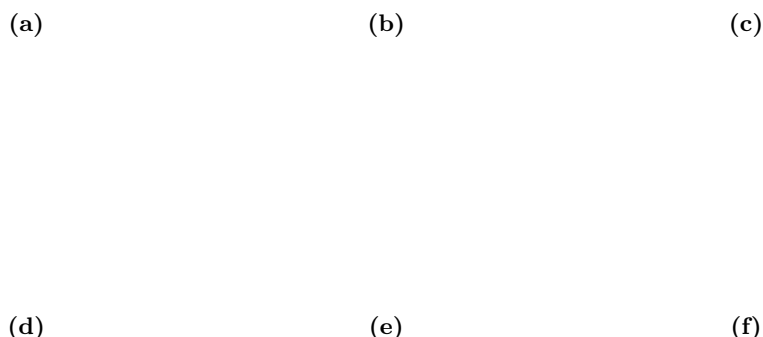


Figure 3: (a) Diffusivity including negative values. (b) Strictly positive diffusivity. (c) Convective velocity converted from negative diffusivity. (d) Effective flux when negative diffusivity is converted to convective velocity. (e) Effective flux when negative diffusivity is discarded. (f) Difference in effective flux when negative diffusivity is discarded.

range. Simulations using MMM-TRANSP of ITER target steady-state, hybrid, and H-mode discharges, from ramp-up through flat-top over a discharge time of 1000 seconds, have been carried out [10, 11]. It is planned to upgrade MMM in the near future to include energetic particle transport effects.

Acknowledgment

This material is based upon work supported by the U.S. Department of Energy, Office of Science, Office of Fusion Energy Sciences, under Award Numbers DE-SC0013977, DE-SC0010661, and DE-SC0021385.

REFERENCES

- [1] RAFIQ, T., KRITZ, A., WEILAND, J., PANKIN, A., and LUO, L., *Physics of Plasmas* **20** (2013) 032506.
- [2] BRESLAU, J., GORELENKOVA, M., POLI, F., et al., *Transp*, [Computer Software] <https://doi.org/10.11578/dc.20180627.4>, 2018.
- [3] RAFIQ, T., KAYE, S., GUTTENFELDER, W., et al., *Physics of Plasmas* **28** (2021) 022504.
- [4] RAFIQ, T., WILSON, C., CLAUSER, C., et al., *Nuclear Fusion* **64** (2024) 076024.
- [5] WEILAND, J., *Stability and Transport in Magnetic Confinement Systems*, Springer, New York, 2012.
- [6] RAFIQ, T., WILSON, C., LUO, L., et al., *Physics of Plasmas* **29** (2022) 092503.
- [7] RAFIQ, T., WEILAND, J., KRITZ, A., LUO, L., and PANKIN, A., *Physics of Plasmas* **23** (2016) 062507.
- [8] RAFIQ, T., BATEMAN, G., KRITZ, A. H., and PANKIN, A. Y., *Physics of Plasmas* **17** (2010) 082511.
- [9] RAFIQ, T., WANG, Z., MOROSOHK, S., et al., *Plasma* **6** (2023) 435.
- [10] RAFIQ, T., KRITZ, A. H., KESSEL, C. E., and PANKIN, A. Y., *Physics of Plasmas* **22** (2015) 042511.
- [11] RAFIQ, T. and WEILAND, J., *Nuclear Fusion* **61** (2021) 116005.